A REVIEW OF NONDESTRUCTIVE TESTING METHODS AND THEIR APPLICABILITY TO POWDER METALLURGY PROCESSING

R. C. O'Brien and W. B. James

Hoeganaes Corporation
Riverton, New Jersey 08077 USA

ABSTRACT

The problem of forming defects in green parts during compaction and ejection has become more prevalent as parts producers have started to use higher compaction pressures in an effort to achieve high density, high performance P/M steels. In this review, several nondestructive inspection methods are evaluated, with the aim of identifying those, which are practical for detecting defects as early in the production sequence as possible.

The most promising NDT methods for P/M applications include electrical resistivity testing, eddy current and magnetic bridge testing, magnetic particle inspection, ultrasonic testing, X-ray radiography, gas permeability testing, and gamma ray density determination. The capabilities and limitations of each of the techniques are evaluated in this review.

INTRODUCTION

In the ceramics industry, the fraction of the finished part cost which arises from scrap due to flaws introduced during processing is estimated to average 50%, and can be as high as 75% (1). While the ceramics industry has been mobilized for the past 15 years towards use of nondestructive evaluation in processing (2), the P/M industry has so far built up only a scattered background of experience.

To remain competitive, P/M parts producers have turned increasingly to simplify processing. It has been shown that the physical properties of P/M parts, especially the fatigue strength, are always improved by increasing the density (3). The need for densification by double pressing can, in many cases, be avoided by pressing to high density in a single step. However, the use of minor problems compared with the introduction of a step or second level in the part. Depending on the severity of the step, a separate, independently actuated punch can be required for each level of the part. During the very early stage of compaction, the powder redistributes itself by flowing between sections of the die cavity. However, when the pressure increases and the powder movement is restricted, shearing of the compact in planes parallel to the punch axis can only be avoided by proper coordination of punch motions. When such shear exists, a density gradient results.

The density gradient is not always severe enough for an associated crack to form upon ejection. However, a low density area around an internal corner, as shown in Figure 2, can be a fatal flaw, since this corner is usually a point of stress concentration when the part is loaded in service.

MICROLAMINATIONS

In photomicrographs of unetched part cross sections, microlaminations such as those shown in Figure 3 appear as layers of unsintered interparticle boundaries which are oriented in planes normal to the punch axis. They can be the result of fine microcracks associated with shear stresses on ejection, which fail to heal during sintering. Because of their orientation parallel to the tensile axis of standard test bars, they have little influence on the measured tensile properties of the bars, but are presumed to be a cause of severe anisotropy of tensile properties.

POOR SINTERING

When unsintered particle boundaries result from a cause other than shear stresses, they are usually present because of insufficient sintering time or sintering temperature, a non-reducing atmosphere, poor lubricant burn-off, inhibition of graphite dissolution, or some combination of these. A severe example is shown in Figure 4. Unlike microlaminations, defects associated with a poor degree of sintering are not oriented in planes.

resolution. The radiation source of the Gamma Densomat is Americium 241 (60 keV). For high-energy beams, Cesium 137 (660 keV) can be substituted.

This method has been shown to be particularly useful in cases where the section of the part to be checked is too small for immersion density measurement (12). Tool life was extended when the method was used for part density checks in order to avoid overloading. Since the radiation source is always decaying, reference parts must be used regularly for calibration of the detected intensity.

ACOUSTIC METHODS

Ultrasonic Testing

Many characteristics of solids can be determined from the behavior of sound waves propagating in them. Ultrasonic signals impinged on a sample at one surface are transmitted at speeds and attenuated at rates determined by the density, modulus of elasticity, and continuity of the material. The sound waves are reflected from other surfaces of the sample, including cracks as well as free surfaces. They can be picked up and amplified for display on a CRT screen.(Figure 9) (7). The height and position of the flaw/defect peak gives an idea of its size and location. While there has been much activity aimed at relating sound propagation to the physical properties of P/M materials, little has been written on the detection of cracks by ultrasonic inspection of porous materials.

Measurements have indicated that the velocity of ultrasonic waves in green compacts is about half the velocity in sintered compacts, and that it is essentially invariant with density (Figure 11) (14,15). It has also been shown that the velocity of ultrasound in green parts is highly anisotropic and that the experimental reproducibility is very poor (Figure 12) (16). It has been proposed that the anisotropy in velocity is due to the orientation of porosity (17). die forced the individual particles together, providing an efficient acoustic coupling between particles.

Ultrasound Transmission in Sintered Parts

Early work relating the physical properties of cast iron to the velocity of sound waves suggested the potential for evaluating P/M steels in the same way (19). As expected, both the velocity of sound in P/M parts and their resonant frequencies have been related to the density, yield strength, and tensile strength. Plain carbon steel P/M specimens were used in one series of tests (14), and the correlation was found to be close enough for the test to be used as a quick check for degree of sintering in production P/M parts. Other work has demonstrated the relationship between sound velocity and tensile strength in porous parts {Figure 14) (20).

The same type of relationships has also been documented in powder forgings (21).

Sintered parts have been found to transmit ultrasound according to the relationships shown in Figure 15 {16). The highest wave velocities occurred in the pressing direction. An additional distinction was found between the velocities in the longitudinal and lateral axes of an oblong specimen, and these results were shown to be reproducible between different powder lots and specimen groups. The anisotropy of velocity diminished at higher densities, and disappeared above 6.85 g/cm^3. detects these variations as distortions in a plastic sheet, which is placed in the path of the plane wave. The information is gathered by a laser which scans a reflective coating on one side of the sheet, as shown in Figure 18 {25).

It would therefore appear that while ultrasonic testing is not appropriate for evaluating green P/M parts, it is applicable to the assessment of sintered components. Careful selection of suitable transducers and their placement is required to obtain the best results as the orientation of defects influences the ability to detect them. Small defects close to the specimen surface can be masked by surface echoes. While enhanced image analysis techniques appear beneficial, it is unlikely that the more sophisticated techniques, such as C-Scan and SLAM will be cost effective for most ferrous P/M parts in the near future.

THERMAL WAVE IMAGING

When a pulsed laser impinges on a surface, the rapidly alternating heating and cooling of the surface is conducted

into the body of the specimen as shown in Figure 20 {30). These "thermal waves" have been shown to possess many of the same characteristics as electromagnetic or mechanical waves: they can be reflected and refracted, they can form interference patterns, and they interact with irregularities contained in the transmitting medium. In coincidence with the thermal wave formation, acoustic waves are formed by the alternating expansion and contraction of the area of impingement of the laser on the surface. These "photoacoustic" waves have the same frequency as the thermal waves (typically 1 MHz), but a much longer wavelength. They are also affected by scattering and reflection of the thermal waves in the volume immediately surrounding the laser impingement point, and it is this effect which allows detection of flaws.

Thermal wave imaging has been used to detect delamination and microcracking in silicon integrated circuits (30).

Another method of detecting interactions of thermal waves with defects is by optical beam deflection ("mirage effect") (31). The impingement point of the laser on the surface heats rapidly, and the air around this point is also heated. If there are no irregularities present beneath the surface, this volume of lower density heated air is roughly hemispherical in shape. A second laser beam which transits this low density air volume by skimming closely parallel to the specimen surface as shown in Figure 21 will be refracted by the density gradient in the same way as it would be by a conventional lens. A four-quadrant detector array gathers the beam deflection data as the specimen surface is scanned by the laser. Subsurface defects are detected as changes in the shape of the density gradient "lens".

While there is no record of thermal wave imaging having been applied to P/M parts, the damping capacity of green compacts would appear to limit the potential application of the technique to sintered components.

Single-Coil Tests

Disruptions in the eddy current path due to any defect that changes the resistivity of the material are detected as extraneous induced voltages in the induction coil. Alternatively, a separate detector coil can be placed in the magnetic field around the test piece.

The alternating current in the induction coil can vary from 1 to 1000 kHz. The depth of penetration varies with frequency, with the highest frequencies yielding the smallest depths ("skin effect") according to the relationships shown in Figure 28 (37).reference part chosen at random from the group to be tested. Differences between the harmonic characteristics of the two parts are displayed as displacement of a dot from the center of an oscilloscope screen; no displacement means the two parts are alike.

Although the magnetic susceptibility of porous sintered steels is reduced by pinning of domain boundary walls by pores, P/M parts are also capable of being analyzed by magnetic bridge comparator. In one study, a set of 120 powder metallurgy production parts was tested in a magnetic bridge comparator. A group of 17 of the parts was singled out on the basis of a displacement of the oscilloscope indication as shown in Figure 31. These parts were tested for chemistry, hardness, crush strength, and pressed height. For comparison, a group of 25 parts selected at random from the remaining body of the specimens were also tested. Statistically significant differences between the groups were found in carbon content and hardness (39). The technique has also been successfully applied to powder forged parts {40).

Although there are no published trials, there is a possibility that the comparator could also work on green compacts.

LIQUID DYE PENETRANT INSPECTION

A liquid which wets the surface of the material being inspected will lower its surface energy by residing preferentially in surface cracks and cavities. In the liquid penetrant inspection technique, cracks are detected by removing the dye from the flat face of the specimen. The dye, which is left behind in the cracks, is then wicked out onto the surface by a fine particulate layer in which the pore radius is even lower than that of the crack. The penetrant in this particulate "developer" layer can be detected visually because of its high contrast with the white developer; or it can be mixed with a dye that fluoresces under ultraviolet light. This process is shown schematically in Figure 33 (42).

Dye penetrant equipment found in P/M shops is generally used only for checking parts of the tooling and machinery for cracks. The dye does not preferentially reside at cracks in P/M parts because the pore radius and the crack radius are equivalent. However, there might be an application to green parts, since the surfaces of green parts are sealed against penetration by liquids both by smearing of the metal powder against the die wall, and by the formation of a thin

coating of dry powder lubricant on the surface. Cracks intersecting the surface may form an opening in this layer that could be detected by dye penetrant.

PORE PRESSURE RUPTURE TESTING OF GREEN COMPACTS

A novel test for detecting ejection cracks in green compacts has been described (43), in which a pressure seal is formed around a corner or area of a part where experience has shown that cracks are likely to occur. The area is then pressurized to about 500 psi using a fixture such as that shown in Figure 34. If a crack is present, the gas pressure in the crack will be sufficient to propagate the crack the rest of the way through the part. This would be classed as a proof test rather than a nondestructive test, since the part is destroyed if defects are present. The test can be used in a nondestructive way on sintered parts: the gas permeability of the pressurized area is measured at reduced pressures. The presence of cracks or low-density areas is indicated by high permeability, as shown in Figure 35.

SUMMARY

The list of NDT methods for which commercial P/M part production histories have been published is short: electrical resistivity, magnetic particle inspection, gas permeability, and gamma ray density determination. An overview of the techniques covered in this review are presented in Table I.

Direct current resistivity testing appears to be a most promising method for testing the integrity of both green and sintered P/M parts {32,33). The technique appears to be capable not only of detecting cracks but also of segregating parts on the basis of hardness and density.

Eddy current testing can be used to detect cracks that intersect the surface of a part but the technique is not suited to finding internal cracks. Corners and edge effects can cause difficulties with eddy current testing as well as with direct current resistivity testing.

Computed tomography and real time X-ray imaging appear to have potential for detecting defects in both green and sintered P/M parts. However, the high cost of the equipment makes it unlikely that these methods will find immediate widespread application in the ferrous P/M parts industry.

Magnetic particle inspection is used to detect surface cracks in sintered P/M parts. However, the technique currently requires an operator to interpret the results and is not compatible with full automation. Advances in imaging techniques (computer vision and pattern recognition) may eventually permit automation of the technique (41).

Gas permeability tests require special fixtures and time to set the part up for testing. The test does not appear to have found widespread application since publication of a paper describing the method in 1970 (43}.

Ultrasonic testing cannot be applied to green P/M parts but is suitable for evaluating sintered parts. Small defects close to corners or the specimen surface can be hard to detect. While enhanced image analysis techniques appear beneficial, it is unlikely that the more sophisticated methods such as C-Scan and SLAM will be cost effective for ferrous P/M parts.

REFERENCES

1) J. W. McCauley, "Materials Testing in the 21st Century", Nondestructive Testing of High Performance Ceramics, Proceedings of 1987 Conference, sponsored and published by the American Ceramics Society and the American Society for Nondestructive Testing, p I

2) R. W. McClung, D. R. Johnson, "Needs Assessment for NDT and Characterization of Ceramics: Assessment of Inspection Technology for Green State and Sintered Ceramics", Ibid, p **33**

3) R. C. O'Brien, "Fatigue Properties of P/M Materials", SAE Technical Paper 880165, March 1988

4) G. F. Bocchini, "High Pressure Compaction, High Pressure Coining, and High Pressure Repressing of P/M Parts", presented at Metal Powder Industries Federation P/M 88 Seminar, "Prevention and Detection of cracks in Ferrous

P/M Parts"

5) F. V. Lenel, Powder Metallurgy Principles and Application, Metal Powder Industries Federation, Princeton, 1980, p 112

6) Metals Handbook, 9th Edition., Vol. 11, American Society for Metals, Metals Park, OH, 1985, p 106

7) C. Rain, "Uncovering Hidden Flaws", High Technology, February 1984

8) B. Chang, et al, "Spatial Resolution in Industrial Tomography", IEEE Trans Nuclear Science, NS30, (2), April 1983

9) H. Heidt, et al, "Nondestructive Density Evaluation of P/M Objects by Computer Tomography", Horizons of Powder Metallurgy, 1986 International Powder Metallurgy Conference Proceedings, Part II, p 723

10) Anon., "Computed Tomography Tackles Nondestructive Testing", Designfax, May 1987, p 66

11) G. Schlieper, W. J. Huppmann, A. Kozuch, "Nondestructive Determination of Sectional Densities by the Gamma Densomat", Progress in Powder Metallurgy, Vol. 43, 1987, p 351

12) C. T. Waldo, "Practical Aspects of the Gamma Densomat", Horizons in Powder Metallurgy, 1986 International Powder Metallurgy Conference Proceedings, Part II, p 739

13) J. t. Rose, M. J. Koczak, J. W. Raisch, "Ultrasonic Determination of Density Variations in Green and Sintered Powder Metallurgy Components", Progress in Powder Metallurgy, Vol. 30, 1974, p 131

14) B. Patterson, C. Bates, W. Knopp, "Nondestructive Evaluation of P/M Materials", Progress in Powder Metallurgy, Vol. 37, 1981, p 67

15) M. F. Termine, "Ultrasonic Velocity Measurements on Green and Sintered P/M Compacts", Hoeganaes Corporation, 1985, Unpublished

16) R. Phillips, W. Franciscovich, "Free-free Resonant Frequency Testing of Powder Metal Alloys to Determine Elastic Moduli", Progress in Powder Metallurgy, Vol. 39, 1983, p 369

17) Y. Xu, S. H. Carpenter, B. Campbell, "An Investigation of the Acoustic Emission Generated During the Deformation of Carbon Steel Fabricated by Powder Metallurgy Techniques", Journal of Acoustic Emission, 3, (2), 1984, **p 81**

18) Rosencwaig, "Thermal Wave Imaging", Science, 218, (4569), 1982, p 223

19) L. J. Inglehart, "Photothermal Characterization of Ceramics", Nondestructive Testing of High Performance Ceramics, Proceeding of 1987 Conference, sponsored and published by the American Ceramics Society and the American Society of Nondestructive Testing, p 163

20) Lewis, "NondestructiVe Inspection of Powder Metallurgy Parts Through the Use of Resistivity Measurements", presented at Metal Powder Industries Federation P/M 88 Seminar, "Prevention and Detection of Cracks in Ferrous P/M Parts"

21) R. A. Ketterer, N. McQuiddy, "Resistivity Measurements on P/M Parts: Case Histories", Ibid.

22) E. R. Leheup, J. R. Moon, "Electrical Conductivity and Strength Changes in Green Compacts of Iron Powder When Heated in Range 50-400°C in Air", Powder Metallurgy, 2-33, (4), 1980, p 217

23) E. R. Leheup, J. R. Moon, "Electrical Conductivity Changes during Compaction of Pure Iron Powder", Powder Metallurgy, 21, (4), 1978, p 195

24) E. R. Leheup, J. R. Moon, "Relationships Between Density, Electrical Conductivity, Young's Modulus, and Toughness of Porous Iron Samples", Powder Metallurgy, 2.-11, (1), 1978, p i

25) Metals Handbook, 9th Edition, Vol. 11, ASM, Metals Park, OH, 1985, pp 76-86

26) P. Neumaier, "Computer-Aided Tester for Nondestructive Determination of Material Properties", Metallurgical Plant and Technology, No. 3, 1987, p 58

27) R. C. O'Brien, "Analysis of Variance of Sintered Properties of P/M Transmission Parts", Hoeganaes Corporation, Unpublished, 1984

28) W. B. James, "Quality Assurance Procedures for Powder Forged Materials", SAE Technical Paper 830364, February 1985

29) Y. F. Cheu, "Automatic Crack Detection with Computer Vision and Pattern Recognition of Magnetic Particle Indications", Materials Evaluation, 42, (11), November 1984, p 1506

30) Metals Handbook, 9th Edition, Vol. 11, ASM, Metals Park, OH, 1985, p 24

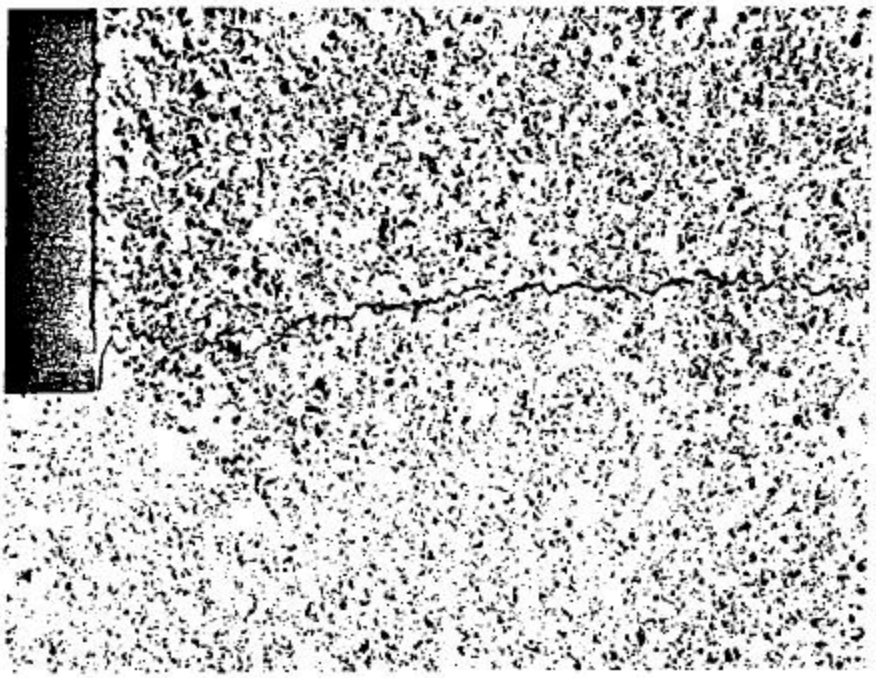

Figure 1: Ejection crack in sintered P/M steel.

30X Unetched

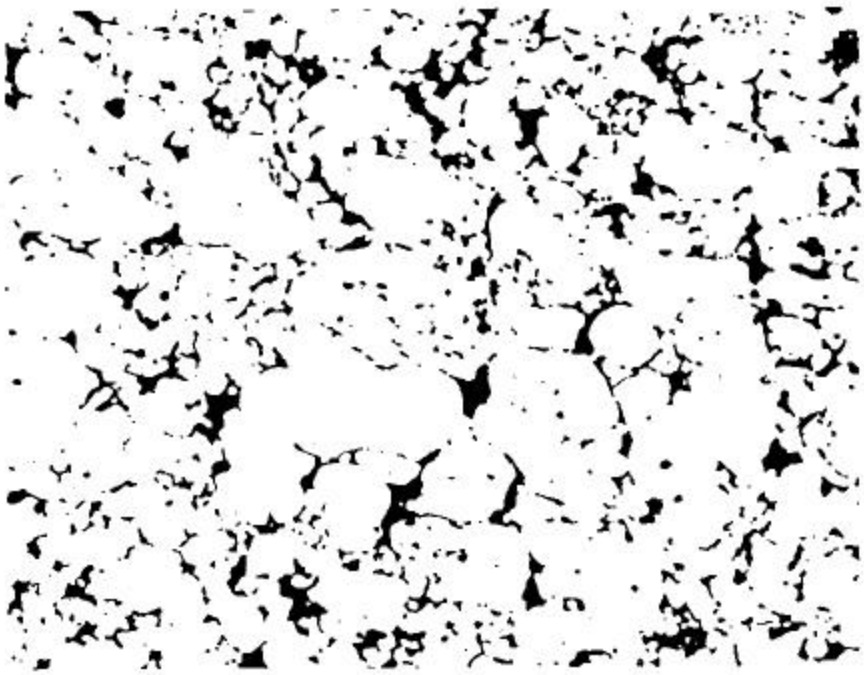

Figure 4: Poor degree of sintering.

100 X Unetched

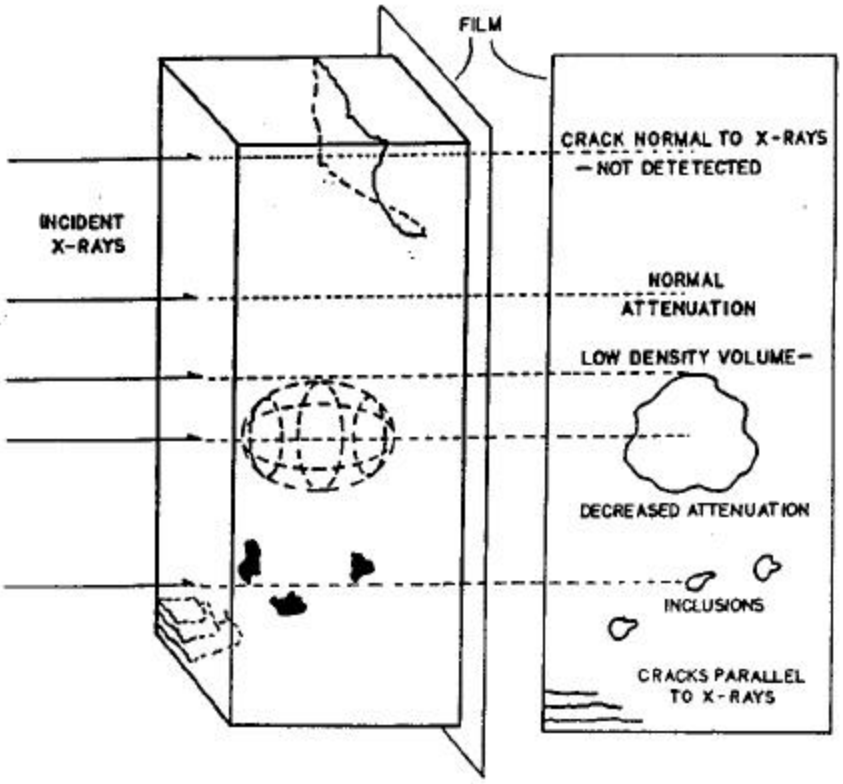

Figure 6: Defect types that can be detected by X-ray radiography are those that change the attenuation of the transmitted X-rays (Adapted from Ref. 7).

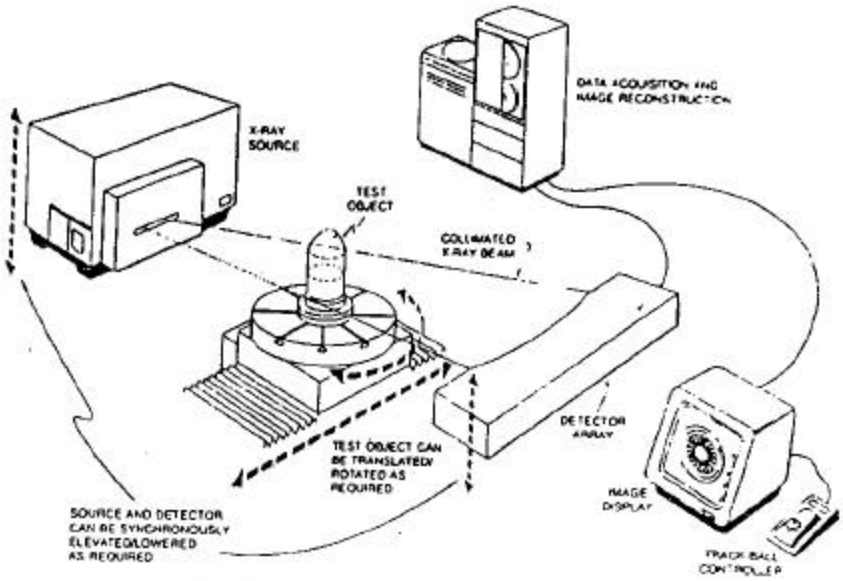

Figure 7: Computed tomography is the reconstruction by computer of a series of tomographic planes (slices) of an object. The transmitted intensity of the fan-shaped beam is processed by computer and the resulting image is displayed on a terminal (8).

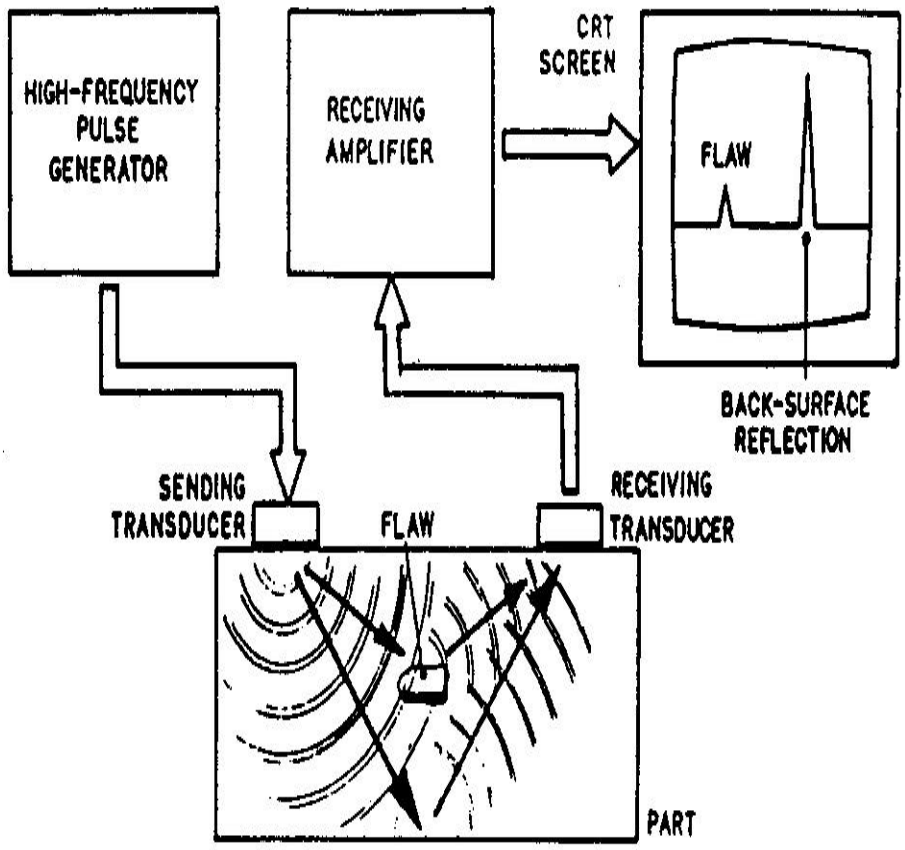

Figure 9: Flaw detection by ultrasound reflection (Redrawn from Ref. 7).

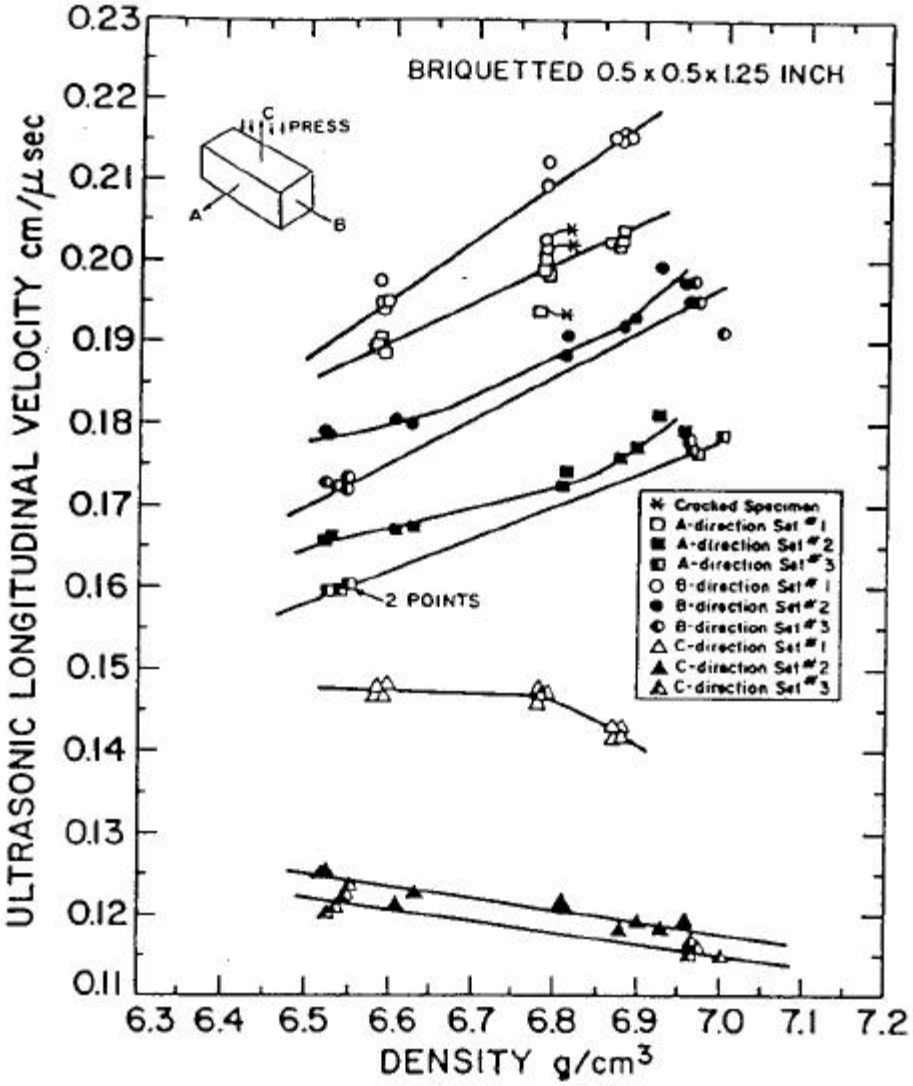

Figure 12: Anisotropy of ultrasound in green T.R.S. bars (16).

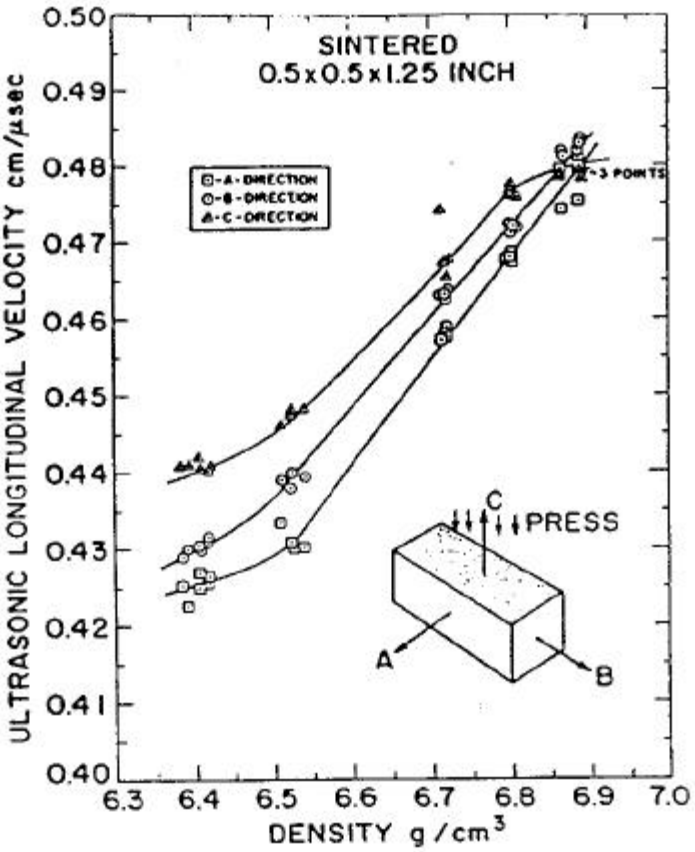

Figure 15: Anisotropy of ultrasound velocity in sintered T.R.S. bars (16).

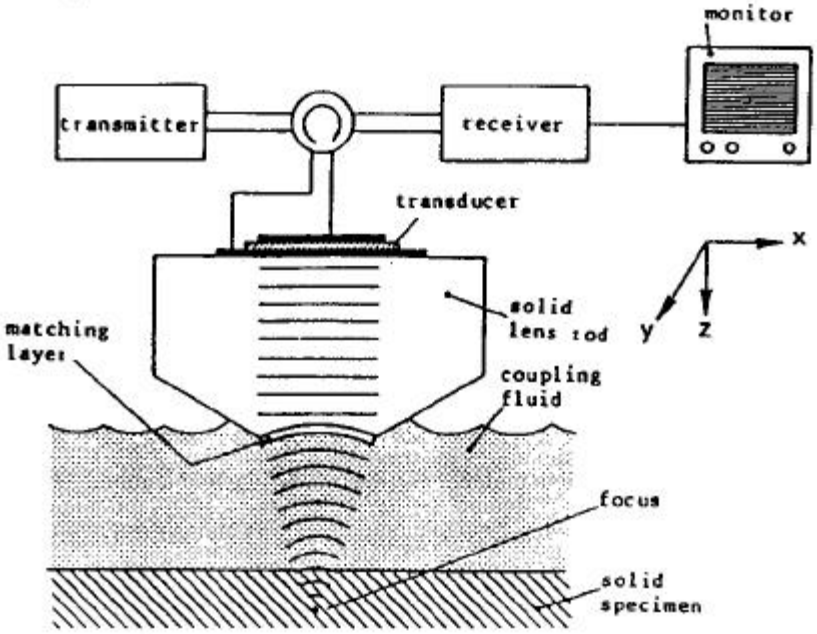

Figure 17: Schematic of the image forming process in scanning acoustic reflecting microscopy (24).

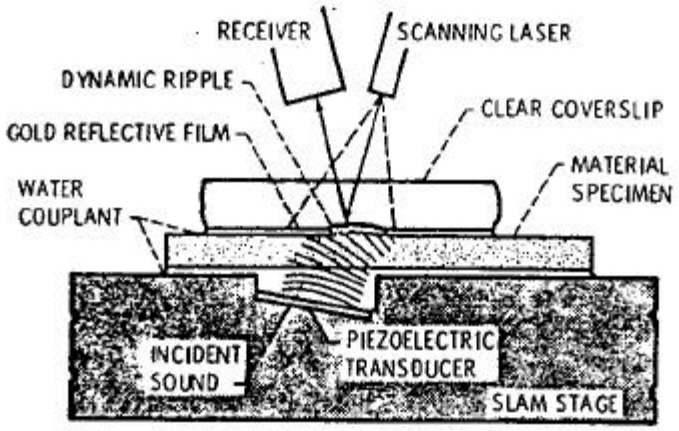

Figure 18: General configuration used in SLAM (25).

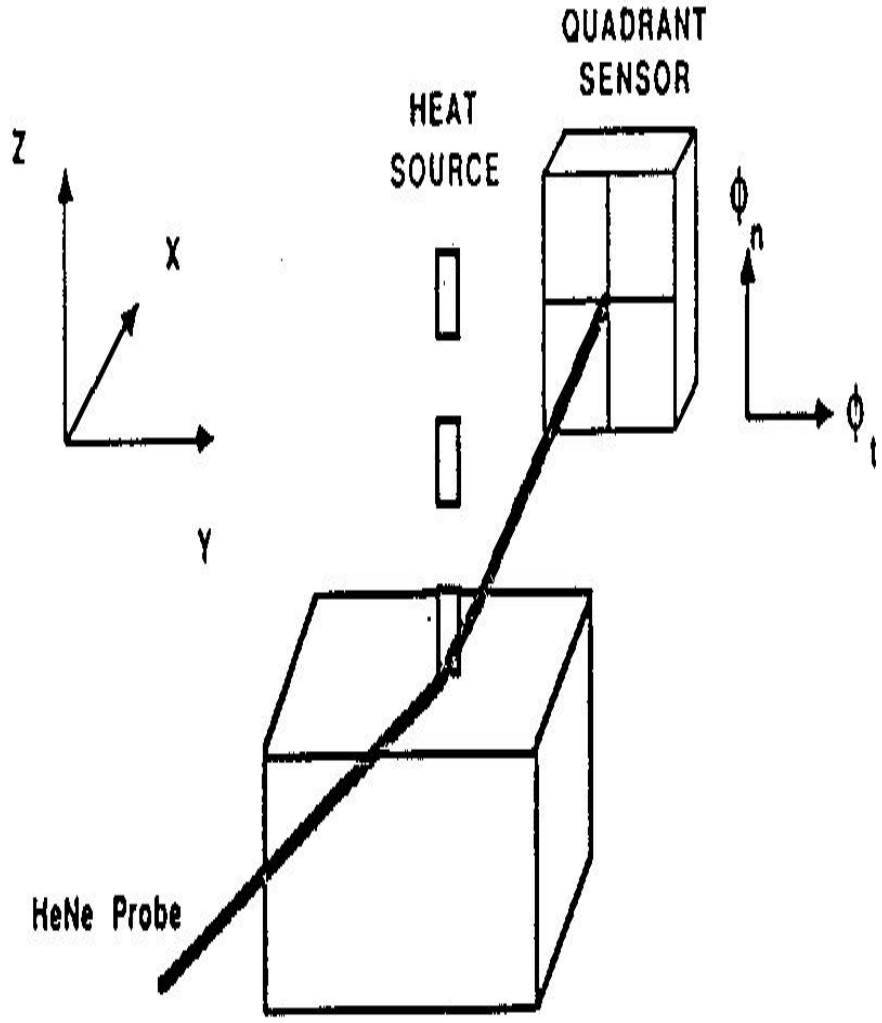

Figure 21: Detection of interactions between thermal waves and flaws by optical beam deflection ("Mirage Effect") (31).

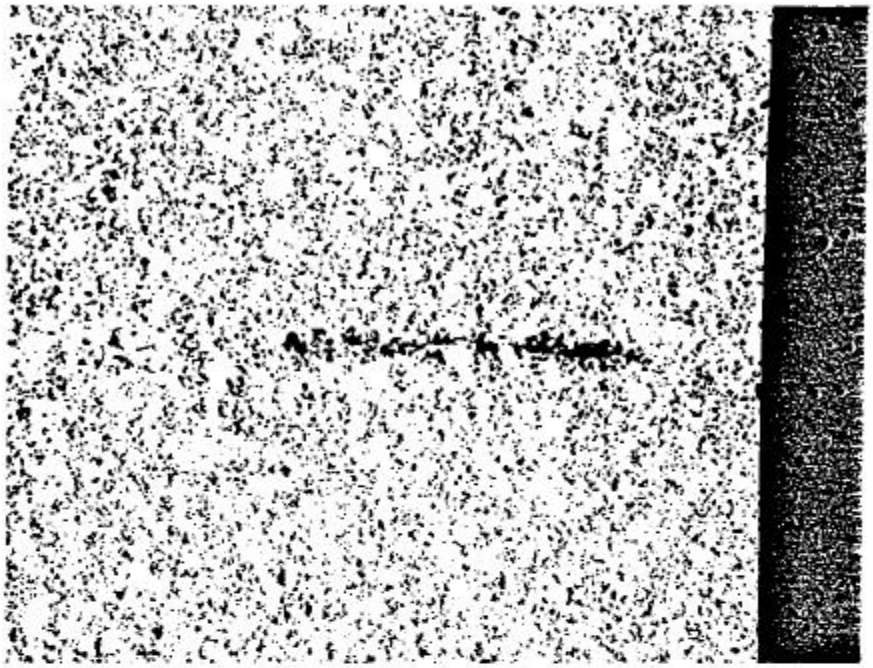

Figure 23: Artificial defect caused by inclusion of a fine wax sliver in the die fill.

30 X Unetched

Figure 24: Artificial defect produced by compacting a partially filled die at 25 tsi, completing the fill, and final compaction of the entire part at 45 tsi.

500 X Unetched

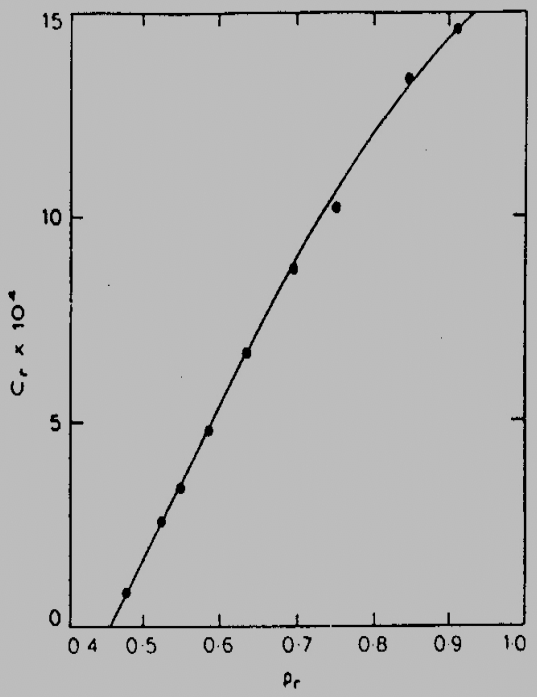

Figure 26: Variation in resistivity with relative density in sintered iron (35).

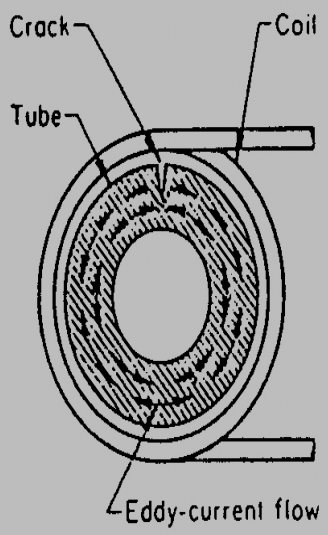

Figure 27: Eddy current test configuration (37).

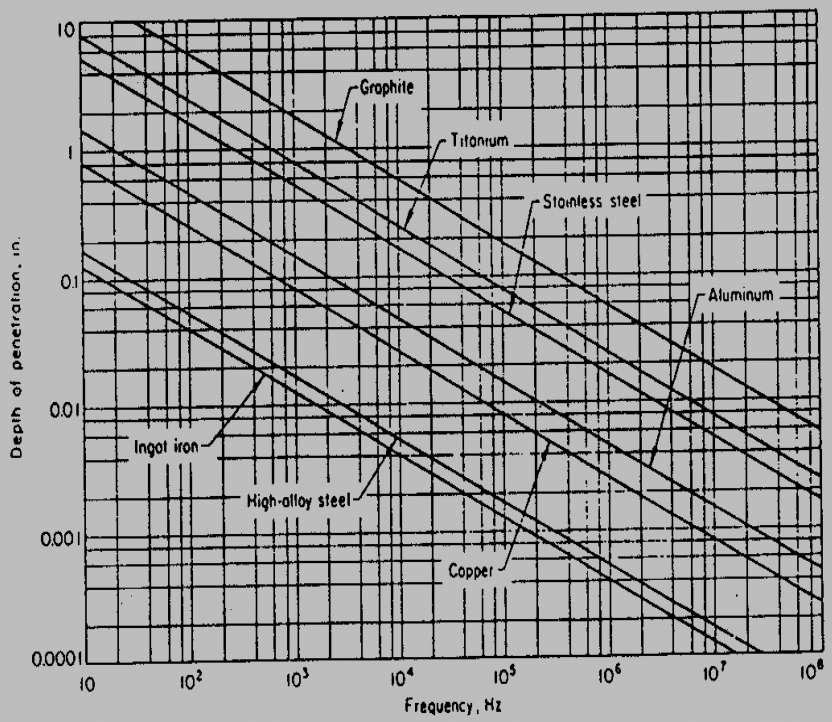

Figure 28: Depth of penetration as a function of frequency for the eddy-current test (37).

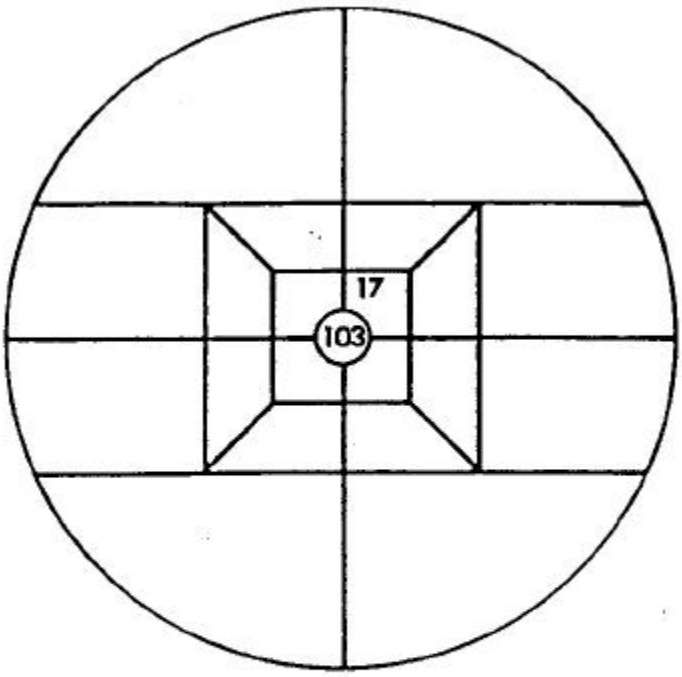

Figure 31: Magnetic bridge comparator display for a set of 120 sintered parts, in which 17 parts were indicated as differing from the reference part (39).

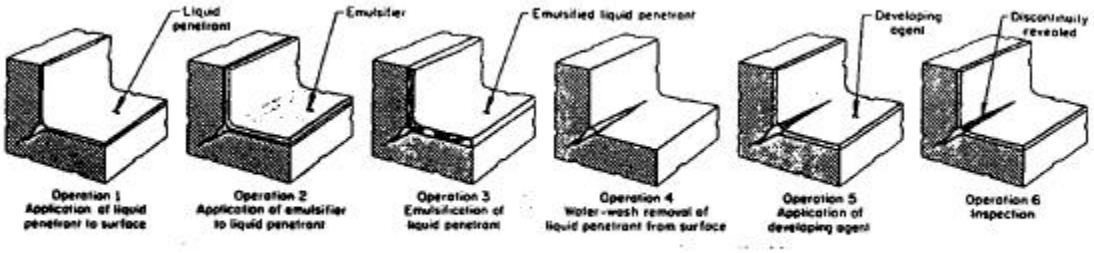

Figure 33: The five steps of liquid-penetrant inspection (42).